

Electronic Supplementary Information for

# ***In situ* AP-XPS analysis of a Pt thin-film sensor for highly sensitive H<sub>2</sub> detection**

Ryo Toyoshima,<sup>a</sup> Takahisa Tanaka,<sup>b</sup> Taro Kato,<sup>b</sup> Ken Uchida,<sup>b</sup> and Hiroshi Kondoh<sup>\*,a</sup>

## **Author address**

<sup>a</sup> Department of Chemistry, Keio University, 3-14-1 Hiyoshi, Kohoku-ku, Yokohama, Kanagawa 223-8522, Japan

<sup>b</sup> Department of Materials Engineering, The University of Tokyo, 7-3-1 Hongo, Bunkyo-ku, Tokyo, 113-8656, Japan

\*To whom correspondence should be addressed.

E-mail: [kondoh@chem.keio.ac.jp](mailto:kondoh@chem.keio.ac.jp)

<b>Index</b>	<b>Page</b>
1. Sample characterization	S2
2. XPS measurement under potential control	S3
3. Quantitative XPS analysis	S4
4. <i>In situ</i> AP-XPS analysis performed at 373 K	S6
5. Thickness of the Pt–H overlayer under working conditions	S7
6. References	S8

## 1. Sample characterization

Fig. S1 shows a wide range XP spectrum taken from the Pt thin-film sensor. The main contribution at 74 eV is identified as the Pt 4f peak. It guarantees that the sample surface is composed of a Pt layer. Additionally, S 2p (164 eV), Cl 2p (200 eV), C 1s (285 eV), N 1s (400 eV) and O 1s (532 eV) peaks are observed. The C, N, S and Cl species are contaminations from the atmospheric environment. C and N species are typical contaminations on the surface, which are derived from organic compounds in the air. The S and Cl contaminations seem to be originating from the substrate cleaning process in the fume hood. Before the Pt deposition, the sample substrate was washed by the piranha solution ( $\text{H}_2\text{SO}_4 + \text{H}_2\text{O}_2$ ). Besides, the SC-2 cleaning process ( $\text{HCl} + \text{H}_2\text{O}_2$ ) is often conducted in the same fume hood. HCl is highly volatile and remains in the environment.

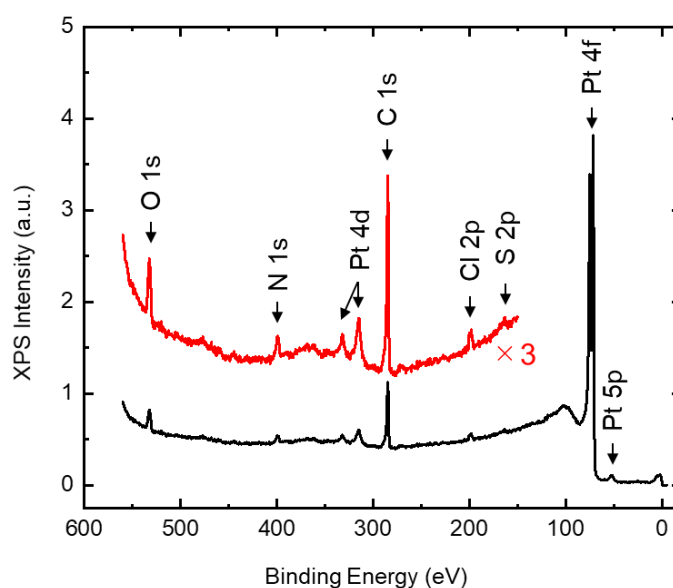


**Fig. S1** Wide range XP spectrum taken from the Pt thin-film sensor. Here the incident photon energy was tuned to 630 eV.

## 2. XPS measurement under potential control

In the present study, the *in situ* XPS measurements were performed under potential control conditions. The influence of voltage application to the spectral shape of XPS was checked (Fig. S2). Here, the Pt 4f XP spectra are compared at two different voltage conditions; 0 V (GND) and 100 mV. As a result, no spectral change was observed between the two voltage conditions.

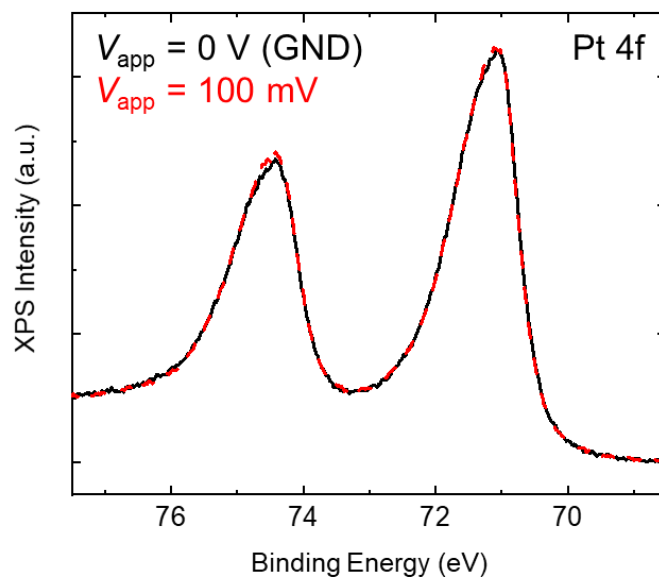


**Fig. S2** Pt 4f XP spectra taken from the Pt thin-film surface. The XP spectra are measured with applying voltages; 0 V (GND) and 100 mV. Here the incident photon energy was tuned to 150 eV.

### 3. Quantitative XPS analysis

The peak intensity is first normalized by the baseline level, then normalized as the overall integrated peak area becomes unity. The binding energy was calibrated with respect to the Fermi-edge. The Pt 4f and O1s XP spectra are curve-fitted to deconvolute into individual components. The XP spectra were curve-fitted via a numerical procedure, where the Doniach–Šunjić function convoluted with Gaussian and the Shirley-type background were applied. The Pt 4f<sub>7/2</sub> and 4f<sub>5/2</sub> levels were fitted simultaneously with an energy separation of 3.4 eV (spin–orbit interaction), where a slightly different Lorentzian width was applied to each component.

The spectral shape of Pt<sub>bulk</sub>/Pt–H component of Pt 4f level is defined by using the fitting result obtained from a clean Pt(111) single-crystal surface. Fig. S3 shows the curve-fitted Pt 4f XP spectra taken from Pt(111) and Pt thin-film surfaces. A component at a lower binding energy side (Pt<sub>surf.</sub>) is associated with a topmost surface Pt. The presence of Pt<sub>surf.</sub> component indicates a clean Pt(111) surface.<sup>1</sup>

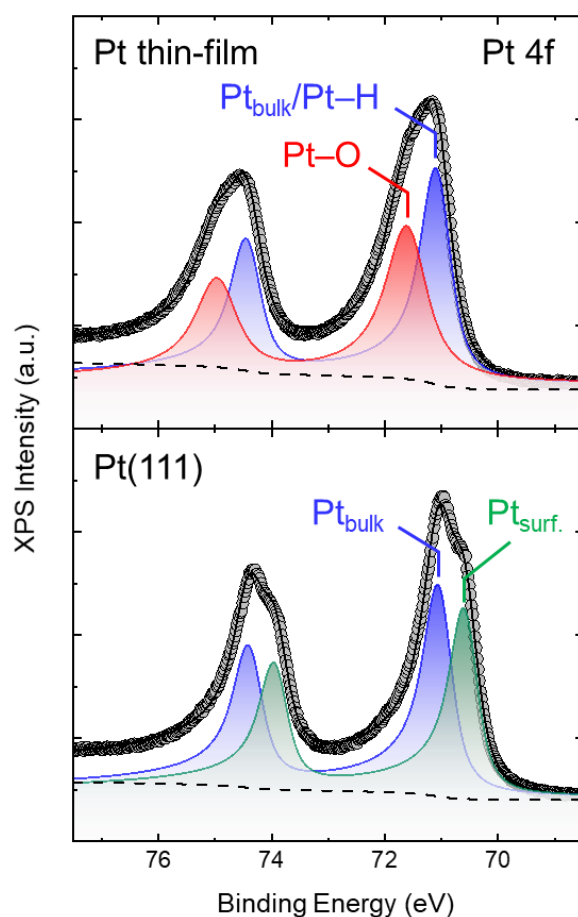


**Fig. S3** Pt 4f XP spectra taken from Pt(111) and Pt thin-film surfaces. Here the incident photon energy was tuned to 150 eV.

In Fig. 3, the time evolution of Pt 4f<sub>7/2</sub> AP-XP spectra at the working condition (100 mTorr H<sub>2</sub>) is shown in parallel with the resistivity change ( $\Delta R/R$ ). The XP spectra are curve-fitted by a numerical procedure as described above. Fig. S4 shows the curve-fitted Pt 4f<sub>7/2</sub> XP spectra, where corresponding resistivity is indicated in each panel. The Pt 4f<sub>7/2</sub> XP spectra are deconvoluted into two components, labelled as Pt<sub>bulk</sub>/Pt–H (blue) and Pt–O (red). The binding energies of Pt<sub>bulk</sub>/Pt–H and Pt–O components are centered at 71.1 and 71.5 eV, respectively. A small deviation of binding energy within  $\pm 0.05$  eV is allowed. It can be seen that the fraction of Pt–O component gradually decreases as the resistivity changes, and the fraction of Pt<sub>bulk</sub>/Pt–H component increases *vice versa* as shown in Fig. S4. It is noted that no other component appears during the H<sub>2</sub> exposure, though the decrease of O-associated species allows formation of Pt–H bond. This supports the present assignment that the 71.1 eV (blue) component is attributed to a summation of the Pt<sub>bulk</sub> and the Pt–H components. This assignment is consistent with the previous XPS results for oxidation of Pt(111) and subsequent H<sub>2</sub> treatment.<sup>3</sup>

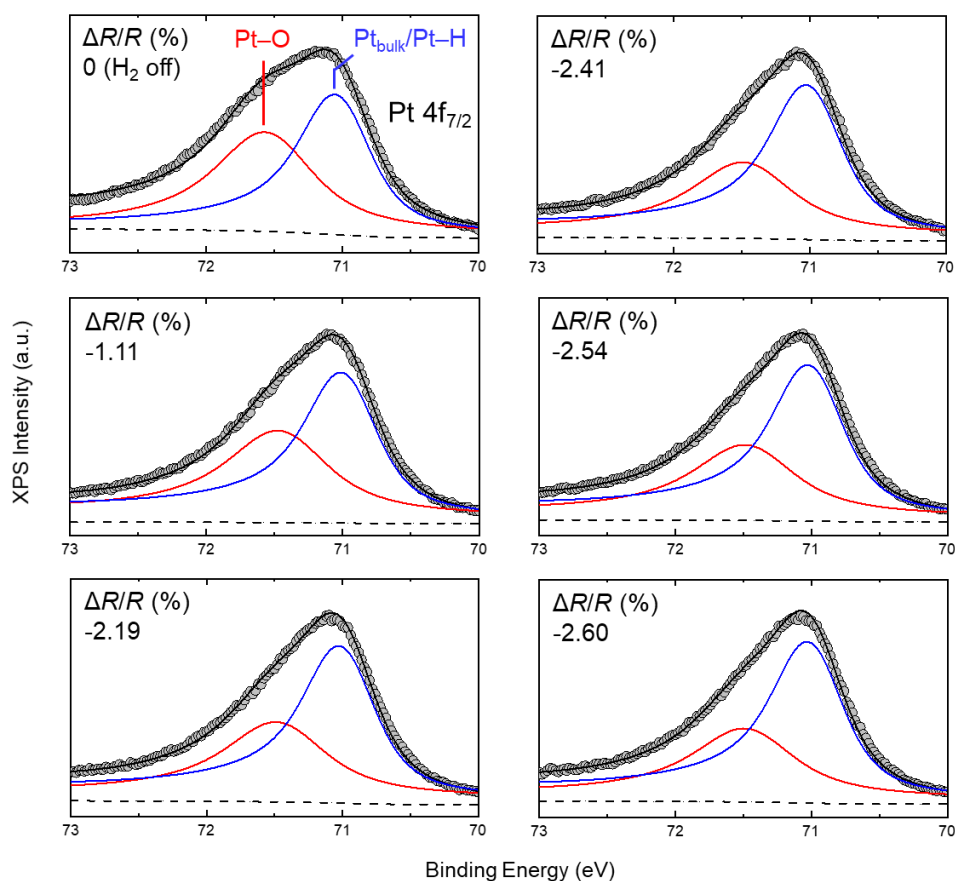


**Fig. S4** Pt 4f<sub>7/2</sub> AP-XP spectra taken from Pt thin-film surfaces at the working condition (100 mTorr H<sub>2</sub>). All the spectra are curve-fitted by a numerical procedure.

#### 4. *In situ* AP-XPS analysis performed at 373 K

The Pt thin-film surface was employed for the *in situ* analysis at working conditions at room temperature (Fig. 2) and 373 K (Fig. S5). Fig. S5(a) shows the time dependence of resistivity under following gas environment; H<sub>2</sub> off, 10<sup>-9</sup> Torr; H<sub>2</sub> on, 100 mTorr H<sub>2</sub> ambient; H<sub>2</sub>/H<sub>2</sub>O on, 100 mTorr H<sub>2</sub> and 100 mTorr H<sub>2</sub>O (gaseous water) ambient. The Pt surface was exposed to 100 mTorr H<sub>2</sub> ambient at time  $t = 0$  s. By introducing the H<sub>2</sub> gas, the relative resistivity ( $\Delta R/R$ ) decreases to about -4.5%. With increasing the surface temperature, the resistivity decreases further.<sup>2</sup> Sensing stability in a H<sub>2</sub>O coexisting environment is an important property of the Pt thin-film sensor. Alternation of resistivity, which is unwanted behavior as sensing material, is about +0.5%, which shows that H<sub>2</sub> can be detected with a high selectivity even under a 1 : 1 gas mixing environment.

Fig. S5(b) shows corresponding Pt 4f and O 1s XP spectra taken at working conditions. As the surface is exposed to the H<sub>2</sub> gas, the Pt 4f peaks are shifted to the lower binding energy side, suggesting the surface is reduced by H<sub>2</sub>.<sup>3</sup> O 1s XP spectra also show a decrease of oxide-associated peak(s) at the working condition. These results are consistent with the result obtained at room temperature. The co-exposing of H<sub>2</sub> and H<sub>2</sub>O causes almost no changes in the spectral shape between H<sub>2</sub> on (blue lines) and H<sub>2</sub> / H<sub>2</sub>O on (black lines) both for Pt 4f and O1s levels. A small hump at 536 eV is assigned as gaseous H<sub>2</sub>O. As mentioned in the main text, the desorption temperature of H<sub>2</sub>O on Pt surface is at 180 K.<sup>4</sup> Therefore, the inference of H<sub>2</sub>O is quite limited on the Pt thin-film sensor.

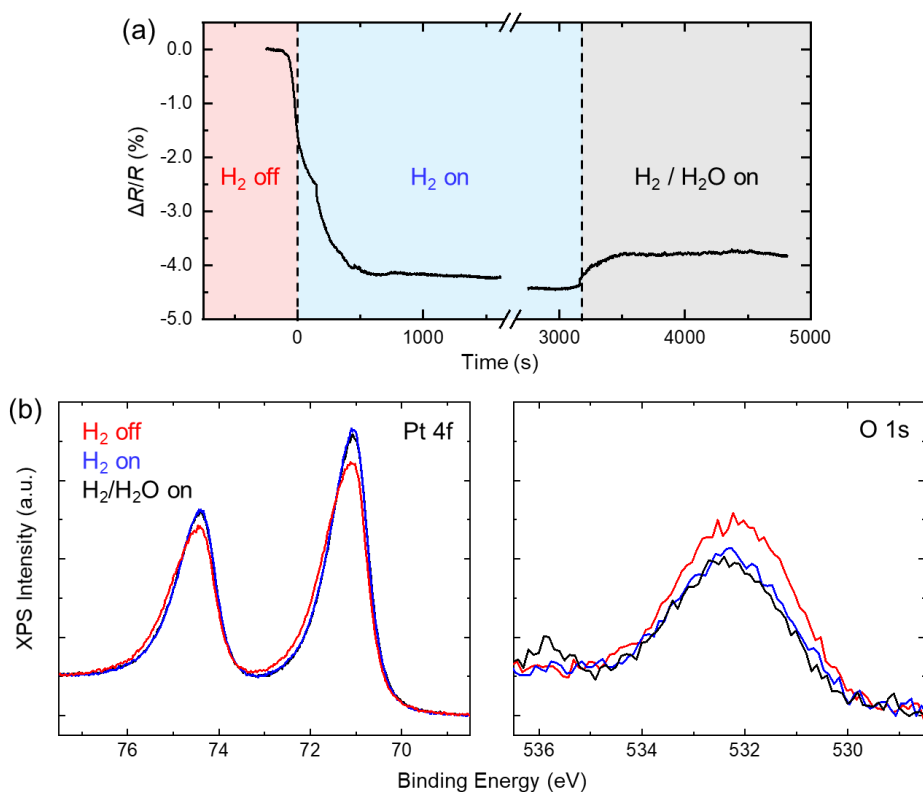


**Fig. S5** *In situ* analysis at working conditions for Pt thin-film sensor surface. (a) evolution of resistivity and (b) Pt 4f and O 1s AP-XPS spectra before (H<sub>2</sub> off) and at (H<sub>2</sub> on) working conditions. At working conditions, the Pt surface was exposed to 100 mTorr H<sub>2</sub> ambient. The surface temperature is 373 K.

## 5. Thickness of the Pt–H overlayer under working conditions

Overlayer thickness  $d$  is quantitatively estimated using XPS peak areas  $I$  of the substrate (S) and overlayer (O) as follows;

$$d = \lambda_0 \sin \theta \times \ln \left( \frac{\sigma_S n_S \lambda_S I_O}{\sigma_O n_O \lambda_O I_S} + 1 \right).$$

where  $\lambda$ ,  $\sigma$  and  $n$  are the inelastic mean free path (IMFP), photoionization cross-section and density, respectively.  $\theta$  is photoelectron emission angle. The thickness is an averaged value on the surface. The Pt–H and Pt–O overlayers are modelled as a Pt–H/Pt–O/Pt stacking layer structure. It is noted that the Pt–O component also contains Pt–C and Pt–N components. The Pt–H component is overlapped with Pt bulk one, thus the intensity is estimated from the difference of peak intensities between with and without H<sub>2</sub>. The bulk component can be assumed to be constant regardless of the ambient environment. Here, the calculation parameters are applied as follows:  $\lambda_S = \lambda_O = 0.40$  nm;  $\sigma_S = \sigma_O = \text{unity}$ ;  $n_S = n_O = \text{unity}$ ;  $\theta = 90^\circ$  (normal emission). The value of  $\lambda$  is calculated based on the Tanuma-Penn-Powell equation.<sup>5</sup>

In Fig. 2 in the main text, under UHV condition before H<sub>2</sub> exposure (H<sub>2</sub> off), the oxide thickness is estimated as 0.25 nm, showing the surface is oxidized in a near-surface region. Under 100 mTorr H<sub>2</sub> ambient (H<sub>2</sub> on), the intensity of Pt–O peak decreased, while the Pt<sub>bulk</sub>/Pt–H component conversely increased. As mentioned above, the increase of peak intensity originated from the formation of Pt–H bond. The calculated thickness of Pt–H layer is about 0.09 nm, therefore the sensor response is driven by a local change of Pt surface in the sub-nm atomistic scale.

## 6. References

- [1] R. Toyoshima, M. Yoshida, Y. Monya, K. Suzuki, K. Amemiya, K. Mase, B. S. Mun and H. Kondoh, *Phys. Chem. Chem. Phys.*, 2014, **16**, 23564.
- [2] T. Tanaka, S. Hoshino, T. Takahashi and K. Uchida, *Sens. Actuators B Chem.*, 2018, **258**, 913.
- [3] D. J. Miller, H. Öberg, S. Kaya, H. S. Casalongue, D. Friebe, T. Anniyev, H. Ogasawara, H. Bluhm, L. G. M. Pettersson and A. Nilsson, *Phys. Rev. Lett.*, 2011, **107**, 195502.
- [4] (a) G. B. Fisher and J. L. Gland, *Surf. Sci.*, 1980, **94**, 446; (b) H. Ogasawara, B. Brena, D. Nordlund, M. Nyberg, A. Pelmenchikov, L. G. M. Pettersson and A. Nilsson, *Phys. Rev. Lett.*, 2002, **89**, 276102.
- [5] H. Shinotsuka, S. Tanuma, C. J. Powell and D. R. Penn, *Surf. Interface Anal.*, 2015, **47**, 871.